LAWRENCE
LIVERMORE
NATIONAL
LABORATORY

LLNL-CONF-642437

TOWARD SINGLE-PARTICLE BIOIMAGING USING X-RAY FREE-ELECTRON LASERS

S. Hau-Riege

August 15, 2013

American Crystallographic Association Annual Meeting
Honolulu, HI, United States
July 20, 2013 through July 24, 2013

Disclaimer

TOWARD SINGLE-PARTICLE BIOIMAGING USING X-RAY FREE-ELECTRON LASERS

Stefan P. Hau-Riege
Lawrence Livermore National Laboratory, P.O. Box 808, 7000 East Avenue, Livermore, CA 94551

ABSTRACT

In this paper we review the recent progress toward single-particle imaging of biological molecules at x-ray free-electron laser (XFEL) facilities. We describe the progression from biological imaging at synchrotrons to imaging at XFELs, discuss recent successes, and point out specific challenges associated with imaging at XFEL facilities.

INTRODUCTION

The ability to emit ultrahigh-peak-brightness x-ray pulses may enable x-ray free electron lasers (XFELs) to revolutionize the field of structural biology. One of the XFEL flagship experiments has been the attempt to determine the structure and dynamics of single biological molecules [1]. In this paper we will review the significant progress that has been made toward this goal since the first hard XFEL, the Linac Coherent Light Source (LCLS) at SLAC National Accelerator Laboratory, has become available in 2009.

Before the advent of XFELs, synchrotrons were the brightest laboratory x-ray sources. It was demonstrated several decades ago that synchrotron radiation can be used to perform x-ray crystallography measurements on protein crystals [2], and it quickly became the work-horse technique for biological structure determination. Initially, protein crystals were typically mm to cm in size. More recently, micro-diffraction techniques have been introduced that allow crystallography experiments on μm-sized crystals [3]. Since, synchrotrons have handed off the baton of developing molecular imaging techniques on ever-smaller structures to XFELs. In the recent years, research groups have been able to demonstrate protein crystallography on nanocrystals and two-dimensional crystals, single-particle imaging, and even first low-resolution imaging of molecules at XFEL facilities. In this paper we will review these recent achievements that build on decades of work performed at synchrotron radiation sources.

REVIEW OF X-RAY—MATTER INTERACTION

The large penetration depth and the short wavelength of x rays make them very well suited for atomic-resolution bioimaging. For example, 10 keV x rays have a wavelength of 1.2 Å, which is on the order of interatomic distances, and a penetration depth of a few mm in biological materials [4], so that multiple x-ray scattering is not a concern. Fig. 1 shows the relative strength of various x-ray—matter—interaction processes as a function of x-ray energy for nitrogen, a common constituent of biological materials. In the regime of 1 to 10 keV that we are considering in this paper, the dominant interaction process is

photoelectric absorption of x rays, which is an ionization process associated with the bound-free transition of an electron. Photoabsorption is the main initiator of x-ray-induced damage to molecules, limiting image resolution and data fidelity. Intra-atomic bound-to-bound excitation and electron free-to-free absorption processes are relatively weak at these x-ray energies.

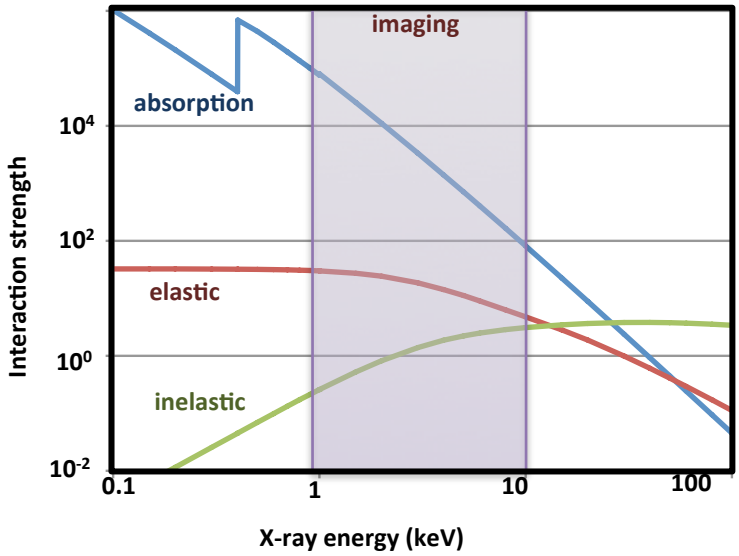

Figure 1: X-ray interaction strength (in arbitrary units) of nitrogen as a function of x-ray energy for different x-ray—matter interaction processes [4].

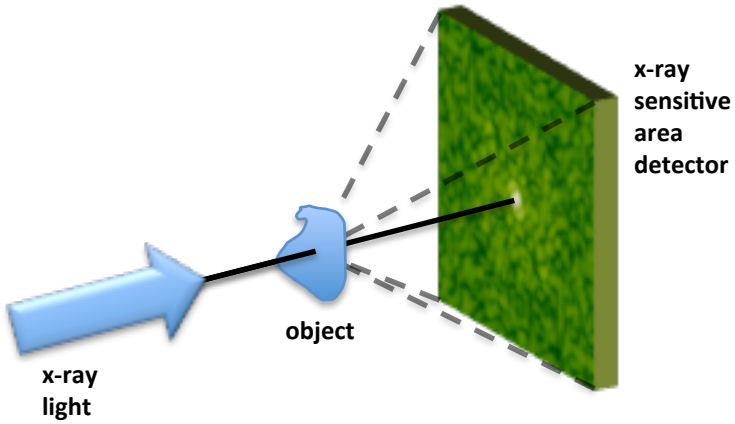

Figure 2: Typical x-ray diffraction geometry.

A typical x-ray diffraction setup is shown in Fig. 2. The diffraction signal that is measured using an area detector originates from the elastically scattered x rays, which is the second strongest interaction process. In this context, elastic means that the x-ray energy does not change during the scattering and that the phase relationship between the incoming and the scattered photons is conserved. Therefore, the area detector measures the intensity of an interference pattern. Some of the interactions of the x rays with the atoms are inelastic in case x rays deposit energy to the sample, contributing to noise in the diffraction pattern and to x-ray—induced damage. Table I summarizes the

contributions from the most important x-ray—matter interaction processes to the damage of the molecule, to the diffraction signal, and to the photon noise. We also included x-ray emission, albeit this tends to be a weak effect in the parameter regime considered here.

TABLE 1

Effect of x-ray—matter interaction processes on sample damage as well as on signal and noise of the diffraction pattern.

Interaction process		Damage	Signal	Noise
Absorption	Bound-free	✔		
	Bound-bound	✔		
	Free-free	✔		
Scattering	Elastic		✔	
	Inelastic	✔		✔
Emission				✔

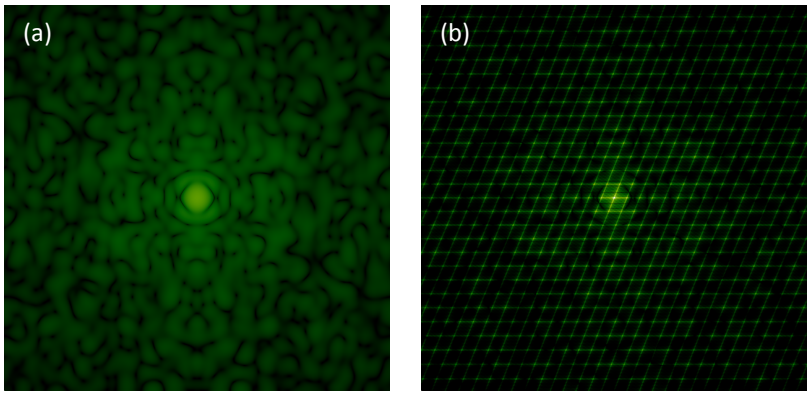

Figure 3: Typical protein diffraction pattern on a logarithmic intensity scale (bright corresponds to high intensity) for (a) a single protein and (b) for a small array of proteins.

STRUCTURE DETERMINATION AT SYNCHROTRONS

Synchrotrons have enabled systematic structure determination of proteins through x-ray crystallography. Fig. 3 (a) shows the calculated diffraction patterns of a single protein. Images like these would be measured in single-protein imaging experiments in the absence of any photon noise. In reality, the diffraction signal from a single protein is so weak that most pixels would not even see a photon. Instead, in x-ray crystallography, copies of identical proteins are arranged in translationally-symmetric three-dimensional arrays (crystals). The periodic arrangement of the proteins leads to intense Bragg peaks in certain directions due to the coherent addition of the scattered radiation, as shown in Fig. 3 (b). In between the Bragg peaks the signal is diminished. By using a crystal, we spread out the radiation dose over a very large number of molecules (on the order of 10^{10}), thereby substantially reducing the detrimental effect of radiation damage. Protein crystallography has been the main characterization technique for structural biology, having provided more than 60,000 entries in the protein database [5]. Roughly 80% of

today's newly determined structures of biological macromolcules are obtained using x-ray crystallography.

X-ray crystallography for structural biology also has its limitations. For one thing, the environment of a protein in a crystal is very different than inside a cell, so that structures determined through crystallography may be artificial. Further, the largest bottleneck for x-ray protein crystallography is growing sufficiently large, high-quality crystals, which is usually a slow and difficult process, and sometimes even impossible. This has led to systematic blank areas in the structural biology databases and often has slowed progress. For example, it took nearly three decades to determine the structure of RNA polymerase II [6].

Before the advent of XFELs, the notion of imaging single molecules instead of crystals was not considered to be a viable option due to their low scattering signal. Increasing the x-ray flux would lead to severe damage, even at cryogenic temperatures. This perception changed once XFELs became available, since these facilities provide extremely bright x-ray pulses that are so brief that they may outrun major x-ray damage processes.

X-RAY FREE-ELECTRON LASERS

The peak brightness of XFELs is about 10^9 larger than for the previously brightest laboratory x-ray sources, namely synchrotrons. The peak brightness measures the number of photons per unit time per area per solid angle and per bandwidth, and it is a figure of merit that is particularly favorable for XFELs. However, even a more neutral measure such as the average brightness demonstrates the strength of XFELs since it is still several orders of magnitude larger than for synchrotrons. Besides the brightness, XFELs offer other unprecedented output characteristics. Current facilities offer tunable x-ray pulses up to 10 keV, pulse durations ranging from 1 to 500 fs, pulse energies of up to 4 mJ, repetition rates of 120 Hz and faster, spectral purity of up to $\Delta E/E \sim 10^{-4}$, and quasi-full spatial coherence. XFELs are becoming available around the world. Currently operating facilities include the soft XFELs FLASH and FERMI and the hard XFELs LCLS and SACLA at SPring8. Numerous other facilities are under construction such as the European XFEL and the SwissFEL, and even more are planned.

The most basic components of an XFEL are an electron source, a linear accelerator, and an undulator. The electron source injects short electron bunches into a linear accelerator in which they are accelerated and compressed in time. The electrons then enter an undulator leading to the emission of synchrotron radiation. If the machine is carefully tuned, the synchrotron radiation is sufficiently intense so that it interacts with the electron bunch, leading to a phenomenon known as microbunching. In this mode, the radiation from the electron bunch is correlated and adds coherently, leading to an exponential rise of the x-ray radiation power as a function of propagation distance in the undulator until saturation occurs. Currently, most XFELs operate in the self-amplified-spontaneous emission (SASE) mode in which the initial synchrotron radiation is not seeded but depends only on the arrival time of the electrons at the entrance of the undulator. The resulting SASE XFEL radiation has only a limited degree of temporal coherence.

SOME FUTURE SCIENCE OPPORTUNITIES OFFERED BY XFELS

Besides biological imaging, XFELs offer numerous other scientific opportunities. Since the pulse duration of XFEL radiation matches many characteristic timescales in matter [7], XFELs naturally enable probing the internal dynamics, which allows us to develop an understanding of reaction pathways, chemical reactivity, and, ultimately, function. Whereas most work at synchrotrons, with numerous important exceptions, of course, has focused on static structure determination, XFELs may enable the recording of (stop-action) movies of atoms and electrons moving in their natural time scale, thereby enabling us, in particular, to better understand structure and function of biological processes such as protein conformation change due to folding, chemical reactions, and magnetic dynamics. XFELs may also enable real-time observation of catalysis, which is one of the backbones of the chemical industry, to watch surface catalysis reactions and determine the transition states in surface reactions and if they can be controlled. It may also become possible to probe the reaction dynamics on fs timescales and monitor electronic and geometric changes to understand surface-mediated chemical reactions. In the field of emergence in correlated materials, XFELs can probe ultrafast electronic order and dynamics, thereby providing an understanding of the processes in which electrons can form exotic quantum phases associated with spin/charge/lattice interactions, such as high-T superconductivity, charge/spin ordering and magnetoresistance, and the fractional quantum-Hall effect.

USING XFELS FOR BIOLOGICAL IMAGING

The potentially game-changing impact of XFELs on structural biology is based on the innovative idea that very short pulses could outrun key damage processes. Conventional steady-state radiation damage limits are 200 photons/Å^2 for 10 keV x rays and 10 photons/Å^2 for 300 eV x rays, beyond which damage modifies the structure on scales of 10 nm and 1 ms. Solem et al. pointed out that images could be collected in a time shorter than it takes for damage to manifest itself [8]. Da Silva et al. showed that single-shot x-ray laser microscopy helps with blurring and allows us to study the dynamics [9]. Neutze et al. suggested that ultrashort XFEL pulses may allow us to step beyond conventional crystallography [10], thereby introducing the concept of diffract and destroy: XFELs with more than 10^6 photons/Å^2 may allow us to obtain single diffraction patterns from large macromolecules, viruses, or cells before they explode. It was suggested to record the individual diffraction patterns of 10^5-10^7 identical particles, classify, average, and orient these patterns, and then reconstruct the electron density, from which the atomic positions can be inferred.

The potential benefit of such single-particle biological imaging would be enormous. For example, it enables the structure determination of proteins which are especially difficult to crystallize, such as membrane proteins which are important for the understanding of living cells and that are key for drug delivery. Currently, less than 300 structures have been determined, and any progress could open up new paths for drug development. Further, such an imaging technique would provide a much faster turnaround and a high

throughput of potentially days instead of years. It may enable time-resolved imaging of processes such as gene expression, DNA repair, and signaling and receptor activation, and it is also very promising for imaging larger objects or objects at lower resolution to understand, for example, the dynamics of larger protein complexes.

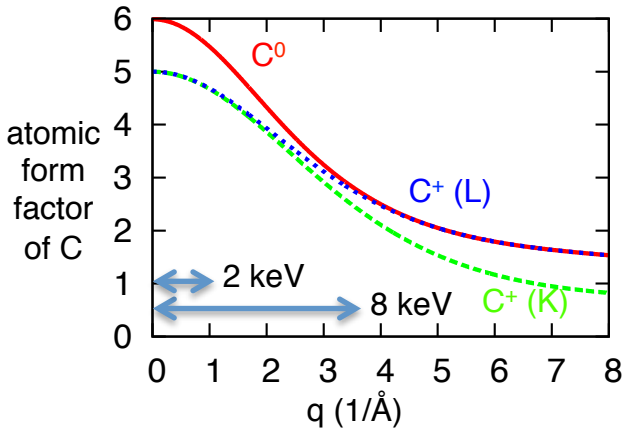

Figure 4: Effect of ionization on the atomic form factor of carbon ions in different ionization states. C^0, C^+ (L) and C^+ (K) correspond to neutral carbon, carbon with a hole in the L shell, and carbon with a hole in the K shell, respectively.

DAMAGE PROCESSES IN XFEL BIOIMAGING

Whereas the initial notion that XFELs could simply outrun radiation damage processes seems very intuitive at first, the transition of a biological particle from a condensed matter system to a nanoplasma is so complex that this needs to be analyzed carefully. XFELs efficiently ionize the atoms and transform molecules into a non-equilibrium nanoplasmas during the x-ray pulse. Ionization damage leads to changes in elastic scattering through modification of the atomic form factor, see Fig. 4, reducing the fidelity of the diffraction pattern. At the same time, ionic motion sets in, leading to changes in the diffraction pattern particularly at high resolutions.

We will now give an overview of the relevant atomic processes. As discussed above, damage is initiated by inner-shell, sequential photoionization that represents about 90% of all x-ray—matter interaction processes, leading to the emission of photoelectrons with kinetic energies of several keV. The resulting ion with a core hole is unstable and will in 95% of all cases decay within a few fs through Auger relaxation, leading to the emission of an Auger electron with an energy of a few hundred eV. Fluorescence decay processes are very weak for the light atoms found in biological materials. The emitted electrons equilibrate through collisional ionization, leading to the emission of electrons with a few eV, and elastic scattering. Once the electron density is sufficiently large, three-body recombination becomes significant. For smaller samples, field ionization takes place at the sample edge. While these atomic processes are proceeding, electron-electron equilibration occurs, and, on a longer time scale, electron-ion equilibration, as well.

Some, but not all, of these atomic processes can be outrun by using shorter pulses. For example, photoionization can hardly be overcome and will lead to changes in the atomic scattering factor. Also, the large speed of the photoelectrons makes it difficult to outrun some collisional ionization processes. Auger decay, on the other hand, is sufficiently slow so that very short x-ray pulses could effectively reduce associated ionization cascades.

The ionic motion during the pulse depends on numerous damage processes, including bond breaking through ionization, ion charge states and local Coulomb repulsion, energy transfer from the slow electron system to the ions, which, in turn, depends on energy transfer dynamics from the photo- and Auger electrons to the bulk of the electrons, and Coulomb charging of the sample. In order to understand the pulse-length dependence of the ionic motion, it is important to understand the energy transfer processes in the sample. The x rays deposit their energy in the photo- and Auger electrons. These fast electrons then transfer their energy to the large system of slow electrons, which, in turn, will heat the ions. A significant amount of energy is stored in the fast photo- and Auger electrons, so that the detailed damage dynamics hinges on the trajectories of the fast electrons and their opportunities to transfer their energy to other slower electrons, all of which, in turn, is affected by charge trapping, electron stopping, and electron scattering.

The electron-electron equilibration dynamics determines the rate of energy transfer from Auger- and photoelectrons to the bulk of the slow electrons [11]. During the pulse, a significant fraction of the absorbed x-ray energy is stored in the fast electrons, leading to a bimodal electron velocity distribution. The slow electrons are in thermal equilibrium among themselves, whereas the fast-electron peak broadens with time and equilibrates due to down scattering and due to an increased temperature of the slow-electrons. This non-equilibrium electron distribution potentially invalidates many thermal-equilibrium theoretical approaches used to describe XFEL damage in the past.

When using smaller samples such as small viruses, single molecules, or thin membranes, space charge effects become more complicated [12]. Escaping photo- and Auger electrons induce charging of the sample that eventually leads to their trapping as illustrated in Fig. 5. On the timescale of an XFEL pulse, trapped electrons can spend a significant amount of time *outside* of the sample. The x-ray absorption profile is not necessarily identical with the heating profile. Hybrid Monte-Carlo—continuum model simulations for x-ray-matter interaction that use an atomic kinetics approach to describe the slow electrons and treats the fast electrons as particles show that the energy transfer depends non-linearly on the pulse fluence [12].

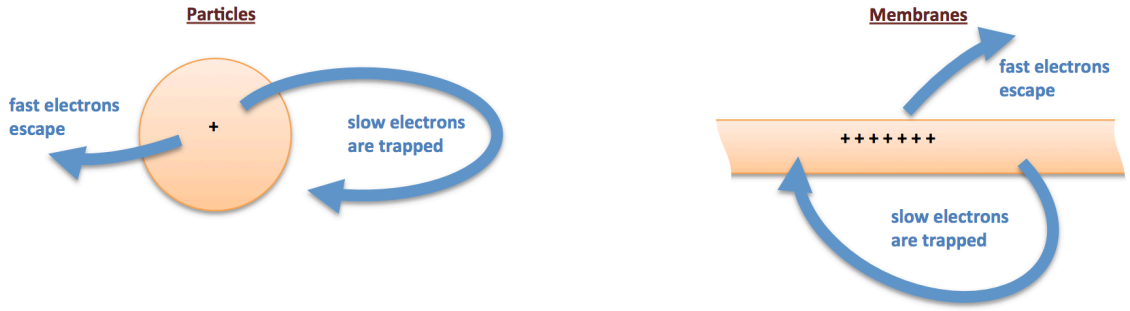

Figure 5: Schematics for trapping of fast Auger and photoelectrons in particles (left) and membranes (right).

FIRST XFEL BIOIMAGING DEMONSTRATIONS

Despite the anticipated radiation damage issues, substantial strides in the development of XFEL structure determination techniques for biological matter have been made over the recent years, in large part due to the lower fluence requirements in crystallography experiments due to Bragg effects, even for small crystals, compared to single-molecule imaging. The first single-pulse nanocrystallography experiment was carried out using a flowing water microjet at the LCLS AMO/CAMP instrument in 2009 [13]. In this experiment, photosystem I (PSI) was taken as a test case, and single nanocrystals that were 0.2 to 1 μm in size were injected into the 3 μm-wide LCLS beam using a 4 μm-wide liquid jet. This technique is also called serial femtosecond crystallography (SFX). The measured patterns were indexed, and molecular replacement was used to reconstruct the structure to a resolution of 8.5 Å. For this test case the structure was known beforehand to 2 Å from traditional x-ray crystallography. These kinds of experiments revealed the interesting effect of "de-phasing" of high-q Bragg peaks once x-ray damage occurs, potentially leading to a self-termination of damage-induced Bragg peak degradation. The details of this effect and its usefulness are still under discussion [14,15].

The resolution of SFX was subsequently improved to 1.9 Å by using 9.4 keV radiation and diffracting from lysozyme microcrystals, which has been well characterized at synchrotrons already. This experiment resulted in good agreement between the electron density maps measured at the synchrotron and measured at the LCLS [16].

More recently, first x-ray diffraction from two-dimensional protein crystals including bacteriorhodopsin (bR) has been achieved, including diffraction from single-layers of bR. Coupling these results to electron microscopy data has provided electron density projection maps, demonstrating clear synergies with cryo electron microscopy [17].

First examples for time-resolved measurements of protein structures were the simultaneous femtosecond x-ray spectroscopy and diffraction measurement of photosystem II at room temperature [18,19]. Also, time-resolved diffraction from photo-excited bacteriorhodopsin in the form of protein crystals has been demonstrated [20].

The first LCLS imaging experiment on non-identical biological particles was performed on single mimiviruses [21] using an aerosol sample injector. General nanoparticle aerosol morphology has been determined through single shot diffraction from airborne particles introduced with aerodynamic lens stack, including soot, airborne NaCl particles, and cluster of spheres [22]. Finally, single, identical biological particles have also been studied at LCLS. The smallest biological single particles seen at the LCLS so far include the viruses in an experiment performed recently by Maia et al. [23].

SUMMARY AND CONCLUSIONS

In summary, near atomic resolution protein structures can be obtained through nano and micro crystallography at LCLS. First at least partially unknown protein structures have been solved. The "Diffraction before destruction" technique holds to 1.9 Å resolution in protein microcrystals. First results on single non-reproducible particles, including viruses and soot aerosols, have been encouraging. Imaging of single molecules will be much more challenging than x-ray nano-crystallography because the signal is much weaker due to the absence of Bragg peaks. This will require larger x-ray fluences, so damage will be an important concern. Other issues include the different orientations of the injected molecules and the need for adjusted data evaluation and reconstruction algorithms, and the required new injection techniques. There is a strong interest in pursuing large membrane-bound protein complexes and other proteins, and successful LCLS imaging of non-abundant membrane proteins will require significant innovations in membrane protein production and nanosample preparation.

ACKNOWLEDGEMENTS

This work was performed under the auspices of the U.S. Department of Energy by Lawrence Livermore National Laboratory under Contract DE-AC52-07NA27344.

REFERENCES

[1] LCLS Conceptual Design Report, SLAC-R-593, 2002.

[2] J.C. Phillips, A. Wlodawer, M.M. Yevit, and K.O. Hodgson, "Applications of synchrotron radiation to protein crystallography: preliminary results", Proc. Natl. Acad. Sci. **73**, 128 (1976).

[3] S. Cusack, H. Belrhali, A. Bram, M. Burghammer, A. Perrakis, and C. Riekel, Small is beautiful: protein micro-crystallography, Nat. Struct. Biol. **5**, 634 (1998).

[4] B.L. Henke, E.M. Gullikson, and J.C. Davis, "X-ray interactions: photoabsorption, scattering, transmission, and reflection at E=50-30000 eV, Z=1-92", Atomic Data and Nuclear Data Tables **54**, 181 (1993).

[5] H.M. Berman et al., "The Protein Data Bank", Nucleic Acids Research **28**, 235-242 (2000).

[6] P. Cramer et al., "Architecture of RNA Polymerase II and Implications for the Transcription Mechanism", Science **288**, 640 (2000).

[7] S.P. Hau-Riege, "High-intensity x-rays – interaction with matter", Wiley-VCH, Weinheim (2011).

[8] J. Solem and G.C. Baldwin, “Microholography of living organisms”, Science **218**, 229-235 (1982).

[9] L.B. Da Silva et al., “X-ray laser microscopy of rat sperm nuclei”, Science **258**, 269 (1992).

[10] R. Neutze, R. Wouts, D. van der Spoel, E. Weckert, and J. Hajdu, “Potential for biomolecular imaging with femtosecond X-ray pulses”, Nature **406**, 752-757 (2000).

[11] S.P. Hau-Riege, Nonequilibrium electron dynamics in materials driven by high-intensity x-ray pulses, Phys. Rev. E **87**, 053102 (2013).

[12] S.P. Hau-Riege, *The role of photoelectron dynamics in x-ray-free-electron-laser diffractive imaging of biological samples*, Phys. Rev. Lett. **108**, 238101 (2012).

[13] H.N. Chapman et al., "Femtosecond X-ray protein nanocrystallography", Nature **470**, 73 (2011).

[14] L. Lomb et al, “Radiation damage in protein serial femtosecond crystallography using an x-ray free-electron laser”, Phys. Rev. B **84**, 214111 (2011).

[15] A. Barty et al., "Self-terminating diffraction gates femtosecond X-ray nanocrystallography measurements", Nat. Photon. **6**, 35 (2012).

[16] S. Boutet et al., "High-Resolution Protein Structure Determination by Serial Femtosecond Crystallography", Science **337**, 362 (2012).

[17] M. Frank et al., “Femtosecond X-ray Diffraction from Two-Dimensional Protein Crystals”, unpublished.

[18] J. Kern et al., "Simultaneous Femtosecond X-ray Spectroscopy and Diffraction of Photosystem II at Room Temperature", Science **340**, 491 (2013).

[19] C. Kupitz et al., *Serial time-resolved crystallography of Photosystem II using a femtosecond X-ray laser*, unpublished.

[20] M. Frank et al., unpublished.

[21] M.M. Seibert et al., "Single mimivirus particles intercepted and imaged with an X-ray laser", Nature **470**, 78 (2011).

[22] M. Bogan et al., unpublished.

[23] F. Maia et al., unpublished.